Using a Wave Model to Study Light Propagation in Emulsion Layers Containing Realistically Shaped AgX Grains

U. Siemen and D. Hertel*

Institute of Applied Photophysics, Technical University Dresden, Germany

It is crucial to take into account the shape and structure of the AgX grains when considering light scattering and absorption in emulsion layers. Most models of light propagation treat photons as corpuscles and grains as spheroids. However, for modern T-grain emulsions this is not a satisfactory approach. Light wave propagation in the vicinity of a grain of arbitrary shape can be calculated from the Maxwell equations of classical electrodynamics, but up until now the computing power required was too great. A new application of multiple-grid algorithms has now been developed that drastically cuts the required computation time from 6 months to less than 10 h for 1 million grid points when solving the equations for a volume element of $(2\ \mu m)^3$. This wave model replaces the MIE model when calculating the cross section of extinction, absorption probability, and angular distribution of light scattering for silver halide grains. Light distribution and internal exposure can be simulated by introducing the layer structure and grain distribution of the real film into the model. Area exposures of up to 0.1 mm^2 are possible with an edge exposure to simulate MTF measurements. A method has been developed to remove granularity noise from simulated and measured MTF test scans.

Journal of Imaging Science and Technology 43: 70–78 (1999)

Introduction

Film structure and processing parameters have enormous influence on the speed and detail reproduction of photographic materials. The effective exposure in the emulsion layer (influenced by internal light distribution), the formation of the latent image (light absorption and quantum sensitivity of the individual grain), and the detection and amplification of the latent image (silver development and dye formation) are all important. Computer models can efficiently simulate the influence of film structure on the recorded image.

Previous publications[1,2] describe a computer model of the photographic process that simulates latent image formation and detection from a given exposure distribution. The resulting spatial microdensity distribution for the image allows the image quality functions to be derived. The three stages of the model are (1) exposure as photon propagation in the emulsion layer and latent image formation, (2) development as latent image detection, and (3) reading the image as an image quality measurement by a densitometer or microdensitometer—directly simulating the physical and chemical processes of producing a photographic image.

Theory

In the first stage of the model, the distribution of incident photons is defined and the photon propagation simulated. The two-dimensional, spatial variant distribution of incident photons covers an area of up to 200 $\mu m \times 500\ \mu m$, that may be extended if required by repetitious continuation. Periodic structures such as sine waves may be exposed onto the film. The simulation can be carried out with arbitrary spectral energy distributions between 380 to 780 nm. Absolute photon numbers of up to 10^6 correspond to absolute exposures between 0.001 and 0.5 lxs. The spectral distributions of reflection, transmission, and absorption are calculated after a sufficient number of photon paths have been simulated.

When modeling light propagation in an emulsion layer, the light scattering and absorption of the individual AgX grains are important. The cross section of extinction, the photon absorption probability, and the angular distribution of light scattering of a single microcrystal depend on the grain shape and structure. These probability functions can only be calculated if simplifying assumptions are made about the shape of the grains, e.g., spherical grains for Mie-scattering. However, when the emulsion contains T-grains the outcome is unsatisfactory.

To solve the problem of light being scattered by a particle of arbitrary shape, the components of the scattered and transmitted waves must satisfy certain boundary conditions. An analytical solution to the Maxwell field equations demands that the particle boundary should coincide with a coordinate plane, which in the case of Mie theory is spherical. Asano and Yamamoto[3,4] extended the Mie model to a spheroidal coordinate system and studied the scattering characteristics of oblate spheroids with aspect ratios down to 1:5. Kurtz and Salib[5] then found that for still lower aspect ratios Asano and Yamamoto's method did not give accurate results. They improved the solution for the boundary conditions and utilized it for AgBr oblate spheroids with aspect ratios down to 1:10. However the approximative approach described here does not demand that the particle boundary should coincide with a coordinate plane. Thus it can be applied to arbitrarily shaped particles, such as the cuboids described in this paper.

Original manuscript received December 26, 1997

* IS&T Member

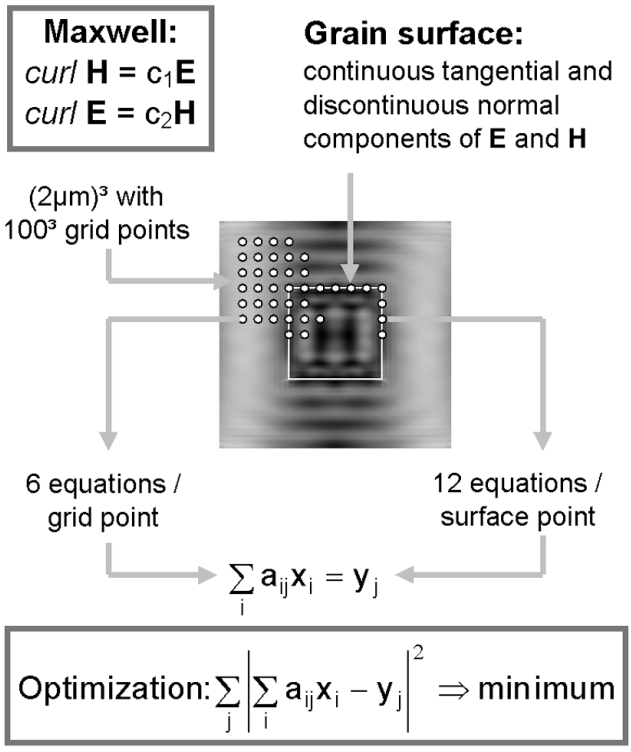

Figure 1. The wave model.

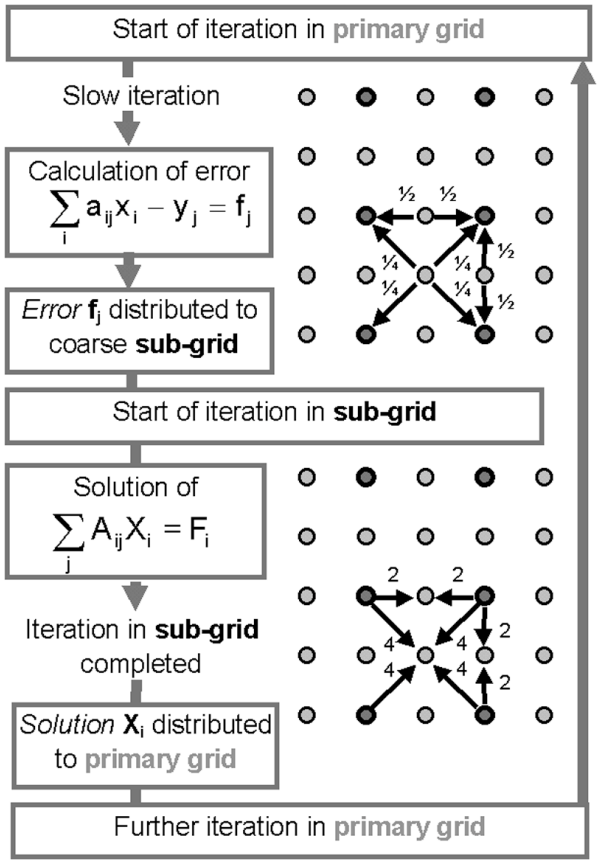

Figure 2. Flow diagram for the multi-grid algorithm.

(i) The Wave Model of Light Propagation. Given enough computing power, light wave propagation in the vicinity of a grain of arbitrary shape can be calculated from the Maxwell field equations.[6] The basic equations for a stationary electromagnetic wave are

$$\text{curl } \mathbf{H} = c_1\mathbf{E}, \tag{1}$$

$$\text{curl } \mathbf{E} = c_2\mathbf{H}, \tag{2}$$

where **E** and **H** are complex vectors whose real parts represent the electric and magnetic fields, respectively, while c_1 and c_2 are complex constants containing physical quantities such as wavelength and complex refraction indices. To solve the coupled differential Eqs. 1 and 2, it is necessary to define volume elements (voxels) containing one grain plus an environment of about one wavelength in each direction. For the chosen voxel, the set of coupled differential equations is then transformed into a set of linear difference equations (see Fig. 1).

The degree of reliability required governs the minimum number of equations needed while the maximum number that can be handled is limited by the available computing power. For voxels of $(2\ \mu m)^3$ with less than 100 grid points in each dimension, about 4.5 million equations are required to achieve a reliability of 85%. To solve such a large set of equations directly (Gauß substitution) would take about 6 months of computing time. Classical methods of successive approximations (Jacobi) are also unsuitable, because the set of equations does not fulfill the criterion of convergence.

However, optimization allows an approximate solution when it is assumed, first, that at the interface between the grain and gelatin the tangential components of **E** and **H** are continuous, and second, that their normal components are discontinuous at the grain surface where there is a change in refractive index. The optimization process would still be very slow, but the application of a multiple-grid algorithm,[7] illustrated in Fig. 2, drastically accelerates convergence of the first approximations and thus reduces computing time. The optimization starts in the primary grid, represented by all the grid points in Fig. 2. After having carried out a fixed, small number i of successive approximations ($i < 4$), the error is calculated for each grid point and then distributed to a coarser sub-grid, represented by the highlighted points in Fig. 2. The numbers against each arrow show the weighting factors used in the transfers between primary and sub-grid. The lower density of grid points in the sub-grid allows a much faster completion of the approximation. The solutions are then redistributed to the primary grid, forming a new, better set of approximate solutions that are then used to continue the process of successive approximations. To illustrate the principle of the multi-grid algorithm, the grids could be transformed into spatial frequencies. In this model the fine primary grid represents the higher spatial frequencies in the wave model, whereas the coarser sub-grids represent the lower spatial frequencies. For the low spatial frequencies (sub-grids), good approximation values can be found quickly, that give better start values for the final approximations at the high spatial frequencies (primary grid). Typically, two or three sub-grids are used in the calculation, which requires 100 Mbytes of memory. The optimization approach combined with the multi-grid algorithm reduces the computing time to about 8 h for a voxel with $97^3 = 912{,}673$ grid points.

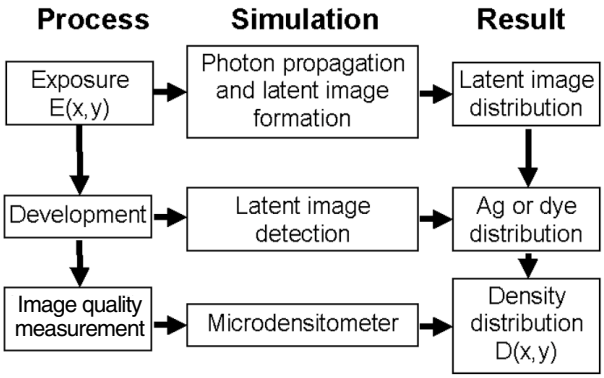

Figure 3. Model of the photographic process.

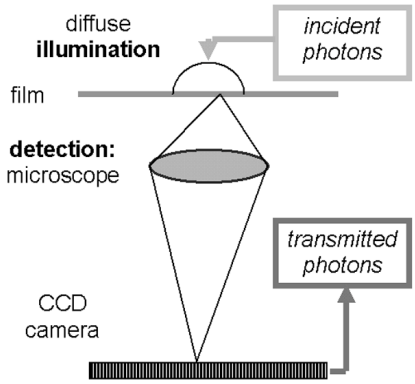

Figure 4. Image quality measurement by means of a CCD-microdensitometer.

(ii) Model of the Photographic Process. This novel wave approach replaces the inadequate Mie model when calculating the probability functions.

Light distribution and internal exposure are simulated by introducing the layer structure and grain distribution of the real film into the model.[1,2] Once a sufficient number of photon paths have been simulated, the spectral distributions of reflection, transmission, and absorption can be calculated. (see Fig 3.)

Knowledge of the absolute number of photons absorbed by the individual microcrystals then allows the latent image formation to be simulated, taking into account both the number of latent image centers per grain and the quantum efficiency (probability that an absorbed photon contributes to the formation of a latent image center). The latent image is detected then amplified by chemical development of silver and by dye formation. The preconditions for a given AgX microcrystal to be developed are the presence of at least one latent image center and the presence of a sufficiently high number of Ag atoms in at least one of those centers. Assuming that the AgX microcrystal develops fully into a compact silver grain, the size of that grain is based on the number of Ag^+ ions in the microcrystal. The result is silver mass as a function of exposure.

(iii) Image Quality Measurement. The structure of the final image is determined by the spatial microdensity distribution, the measurement of which requires a scanning microdensitometer. The Monte Carlo simulation of photon propagation in the developed film provides the microdensity distribution of the recorded image. The optics of the microdensitometer and densitometer are simulated using realistic parameters. For example, sample illumination can be specular or diffuse. Different directional distributions (numerical apertures) and spectral distributions (visual or Status A/M) can be used to detect the transmitted photons. To simulate a CCD microdensitometer, the transmitted photons are registered by an array of pixels as shown in Fig. 4.

(iv) Noise Removal. The spatial microdensity distributions resulting from the simulation (i) - (iii) are distorted by noise from two differing sources. First, the calculations are carried out on only relatively small areas of film, $(200\ \mu m)^2$. Second, edge exposures on real films are scanned by a microdensitometer with only a relatively small measuring slit, $(2 \times 100)\mu m^2$. As a consequence, the signal-to-noise ratio is low and noise removal is an essential part of data processing when calculating MTF from the scans.

TABLE I. Emulsion Data

Emulsion type	mono	T-grain	
Grain diameter [μm]	0.53	0.80	1.06
Aspect ratio (T-grain)	—	1:6	1:8
Ag laydown [g/m^2]	1.4	3.56	0.4
Layer thickness [μm]	4.4	10	1.6

When a sharp edge is copied onto a color negative film, the maximum curvature of the signal (edge image) is of the same order as that caused by granularity noise. Therefore smoothing algorithms with a fixed width smoothing window are unsuitable, because they cannot differentiate between signal and noise. MTF values would be lowered considerably if the slope and profile of the edge were too vigorously smoothed.

To remove the noise without deteriorating the signal, a smoothing filter with a variable window has been developed. This window is narrowest at the edge, the position of which is given by the maximum of the first derivative of the signal. The width then gradually increases with increasing distance from the edge.

Experimental

The calculations have been performed for three model AgBr emulsions, one with monodisperse cubic grains and two with T-grains. Both emulsion types were based on color negative emulsions and coated as single layers. Table I details the experimental coatings.

Spectral reflection, transmission and absorption for the unexposed layers were obtained using a Shimadzu UV-VIS-NIR 3100 spectrophotometer. The cross sections of extinction and the absorption probabilities were then calculated using the diagrams from Metz.[8]

The test patterns for the image quality measurements (step wedges for characteristic curves, edges with contrasts between 0.23 and 0.6 for MTF) were exposed onto film samples using a sensitometer with simulated daylight.

To ensure that the maximum number of latent image centers were completely developed into compact Ag grains, gold latensification, wash in 0.1% KBr followed by Kodak KRX developer was chosen.[9]

The visual optical densities were measured with a Macbeth TR 924 densitometer.

The edge images were scanned by a computer-controlled microdensitometer using a photodiode line with 1024 slit-shaped pixels.[10] MTF was calculated from the edge scans after correcting them with the characteristic curve and noise removal.

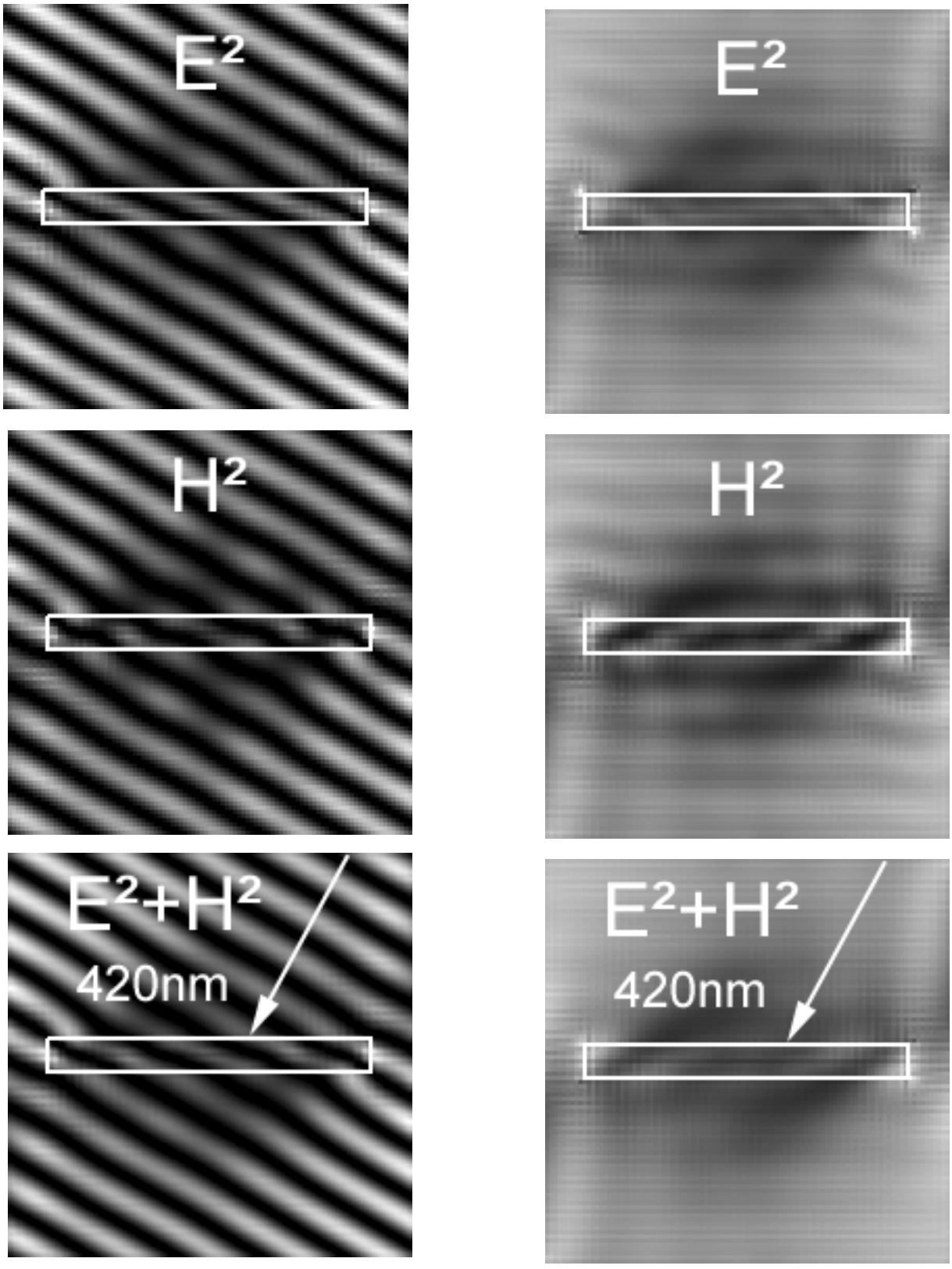

Figure 5. Propagation of a light wave at 420 nm through a T-grain in voxel of $(1.27\ \mu m)^3$; spatial distributions of electric field energy $\mathbf{E}^2$, magnetic field energy $\mathbf{H}^2$, and intensity ($\mathbf{E}^2 + \mathbf{H}^2$), instantaneous (a) through (c) and averaged over time (d) through (f).

Results and Discussion

With the development of this method of simulating light propagation, it is now possible to compare new results obtained using the wave model with those previously reported[1] for the monodisperse cubic emulsion based on Mie theory. The use of a statistical model in simulating the subsequent steps of latent image formation and detection is described in the previous publication.

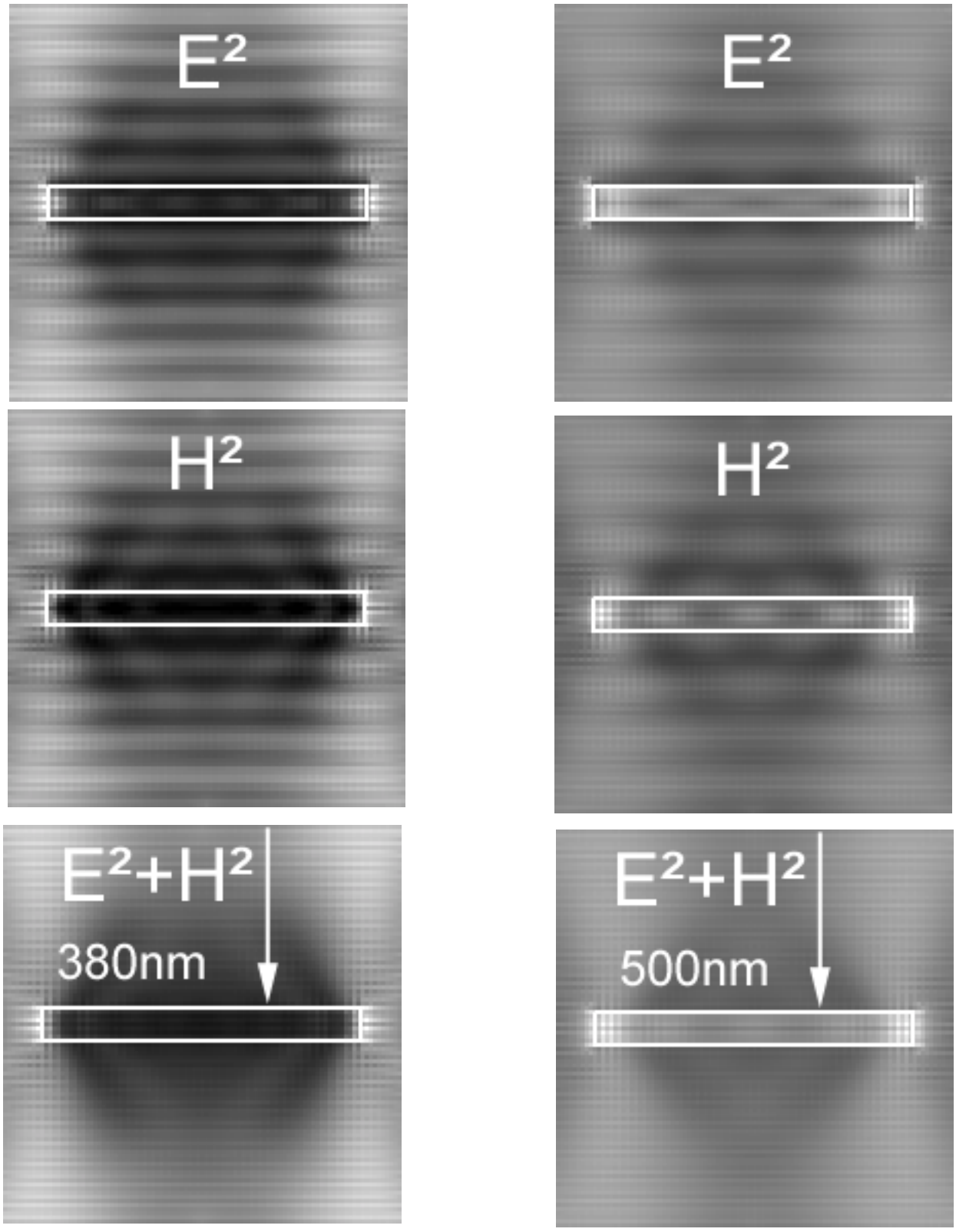

Figure 6. Light propagation through a T-grain (1.06 μm) at 380 (a) through (c) and 500 nm (d) through (f), 90° angle of incidence.

(i) The Wave Model of Light Propagation. The same T-grain emulsion previously discussed[1] (grain diameter 1.06 μm, aspect ratio 1:8) was again used to assess the value of the wave model. Figures 5(a) through 5(c) show the instantaneous spatial energy distributions of electric field energy E^2, magnetic field energy H^2, and intensity ($E^2 + H^2$) for a light wave at 420 nm in a voxel of $(1.27\ \mu m)^3$ containing a T-grain in gelatin. The arrow indicates the direction of movement of the wave front; the lighter the image, the higher the energy level. A 60°

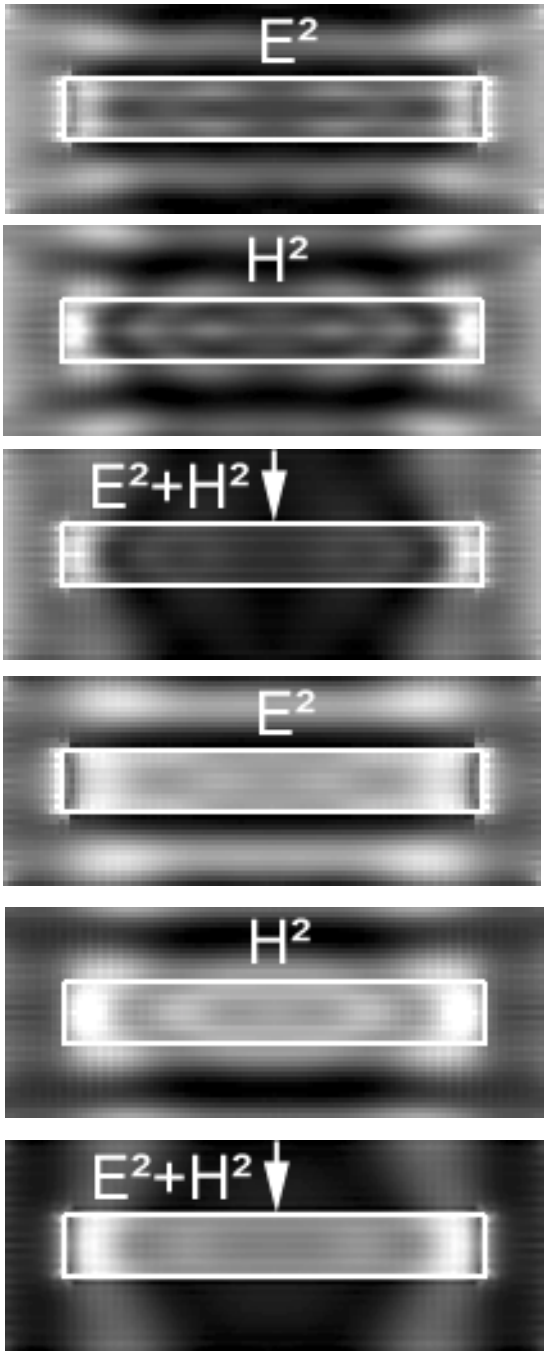

Figure 7. Light propagation through a T-grain (0.8 μm) for 380 (a) through (c) and 500 nm (d) through (f).

angle of incidence to the grain surface offers a better view of wave propagation through the grain. Figures 5(d) through 5(f) record spatial distributions averaged over time for the same grain, volume element, and incident light wave.

To calculate the optical properties of the grain (cross section of extinction, absorption probability, and angular distribution and cross section of light scattering) as a function of wavelength, the simulations have to be carried out at different wavelengths within the sensitivity range of AgBr. Figure 6 gives the field and intensity distributions averaged over time for light waves at 380 and 500 nm with a 90° angle of incidence.

Additional simulations for the T-grain emulsion containing 0.8 μm grains with aspect ratio 1:6 proved that reducing the size of the voxel could further shorten computation times with no loss of accuracy (Fig. 7).

Similar simulations of light propagation have been carried out for voxels of $(1.40\ \mu m)^3$ containing cubic grains in the monodisperse emulsion. Figure 8 shows the field and intensity distributions averaged over time for light waves at 380 and 650 nm with a 90° angle of incidence.

The field and intensity distributions shown above were simulated using 97 grid points per dimension of the voxel, with 2 or 3 sub-grids for optimization. Whether further iterations and sub-grids are needed depends on the intermediate results, which must be carefully monitored. When using an IBM RS6000/39H computer with 128 Mbytes RAM, computation time was about 8 h.

(ii) Model of the Photographic Process. The cross section of extinction, the absorption probability, the angular distribution and cross section of light scattering can all be calculated from the spatial intensity distributions in the vicinity of the AgX grains.

For the monodisperse emulsion there is good agreement between the angular distributions of light scattering calculated from the Mie theory and those from the wave model (Fig. 9).

The fine structure in the curves at angles greater than 30° is attributable to statistical fluctuations in the simulation. However the distinct peak at 150° in the wave model curve is more problematic. It is thought to result from backscattering due to the cubic shape of the grain. Unfortunately the light scattering experiments on a single grain that would have proved or disproved this theory could not be carried out because the emulsions were not available in liquid form. The emulsions were available only as coatings where multiple scattering cannot be avoided.[11]

The spectral distributions of the probability of absorption (Fig. 10) and the cross section of extinction (Fig. 11) were calculated from coating data and optical measurements (transmission, reflection, and absorption).

For the monodisperse emulsion, the curves of absorption probability show good agreement between the two models and also with values obtained by Klein[12] from measurements on a monodisperse emulsion of similar grain size.

While both Q_{ext} curves in Fig. 11(a) display a similar minimum value at a similar wavelength, typical for spheres larger than 0.2 μm, the models are not in agreement on either side of the minima. At shorter wavelengths, the region of greatest sensitivity for AgBr, the wave model predicts higher values that are a better fit to the curve calculated from the measured spectral transmission $T(\lambda)$ than the Mie model, whereas at longer wavelengths the situation is reversed and the Mie theory predicts higher values that are a better fit to $T(\lambda)$.

Metz[13] and Berry[14] have previously observed the poor fit between curves calculated from Mie theory and experimental data on the short wavelength side of the minima in Q_{ext}. It was attributed to uncertainties in determining the grain size and the influence of multiple scattering. At wavelengths greater than at the minima in Q_{ext}, the discrepancy between $T(\lambda)$ and the results from the wave model could be due to the influence of sensitizing dyes.

No experimental data are available in the literature regarding the optical behavior of T-grains. Figure 11(b) shows the cross-sections of extinction and scattering

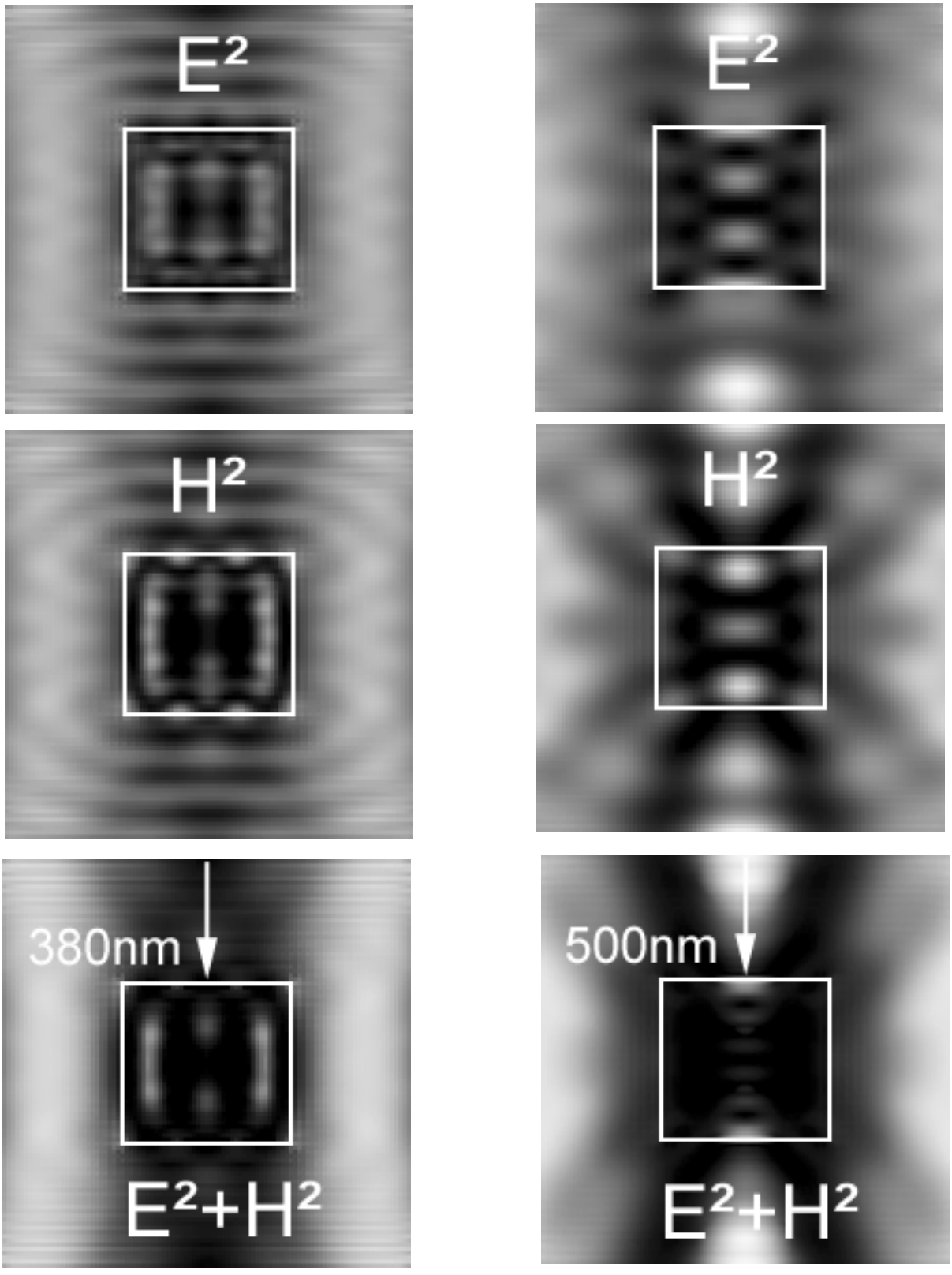

Figure 8. Light propagation through a cubic grain of diameter 0.53 μm at 380 (a) through (c) and 500 nm (d) through (f), 90° angle of incidence.

calculated for the two T-grain emulsions. For 1.06 μm grains there is a good agreement in the region of AgBr's greatest sensitivity to light, between Q_{ext} values obtained from the wave model and from measured $T(\lambda)$. At wavelengths above 500 nm the discrepancy between the curves could be again due to the influence of sensitizing dyes used in color negative film emulsions.

After simulating the complete photographic process as described previously,[1] varying the statistical parameters of latent image formation and detection, the curves of sil-

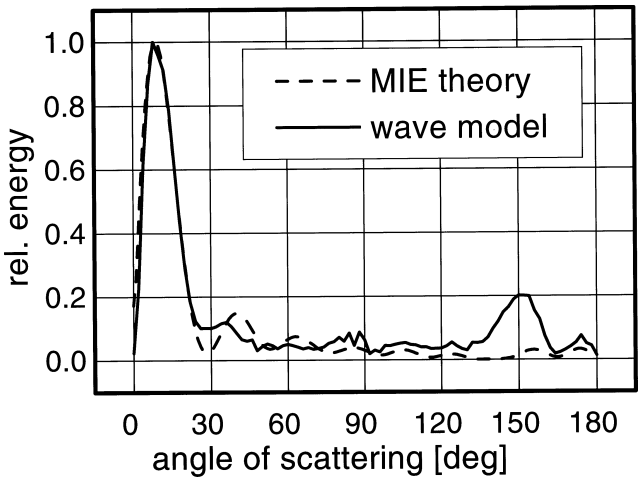

Figure 9. Angular distribution of light scattering at 380 nm, monodisperse emulsion.

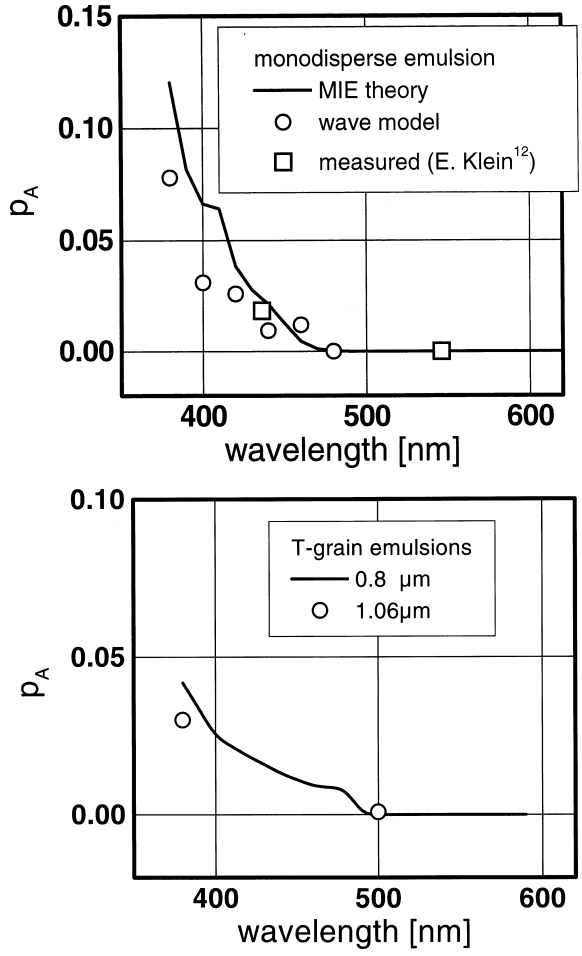

Figure 10. Probability of absorption: monodisperse emulsion (a) and T-grain emulsions (b).

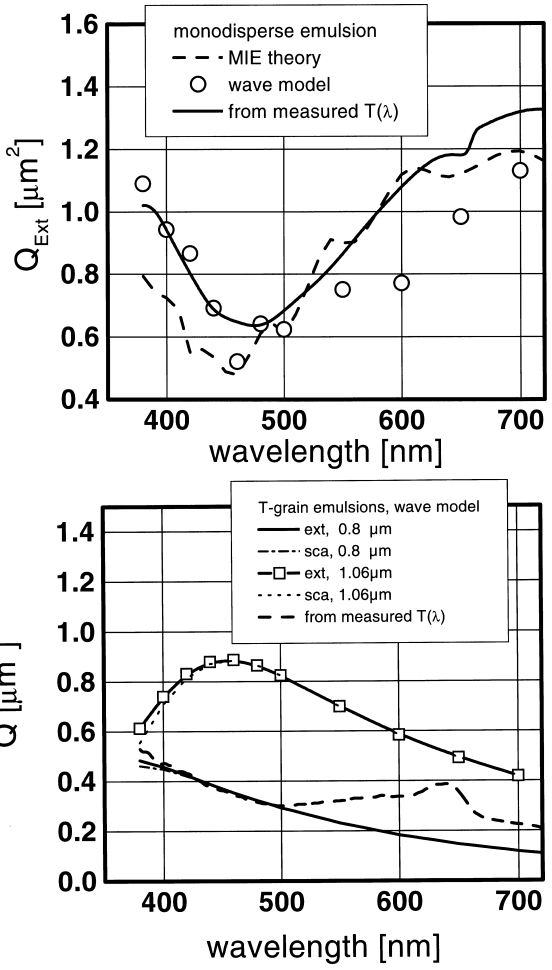

Figure 11. (a) Cross section of extinction, monodisperse emulsion. (b) Cross sections of extinction and scattering, T-grain emulsions.

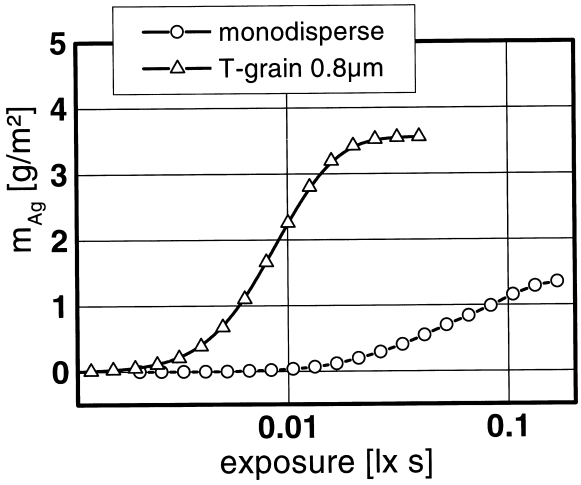

Figure 12. Calculated silver mass as a function of exposure, calculated for monodisperse and T-grain emulsions.

ver mass as a function of exposure could be calculated.

Figure 12 shows that the simulated T-grain emulsion has higher sensitivity and steeper gradient than the monodisperse emulsion.

(iii) Image Quality Measurement. To simulate the determination of MTF, the distribution of incident photons was defined as a sharp edge (contrast 0.6) covering an area of 200 μm × 500 μm. The spectral energy distribution of the incident photons was the same as that of the sensitometer (simulated daylight).

After simulation of the photographic process (ii) the resulting two-dimensional microdensity distribution was

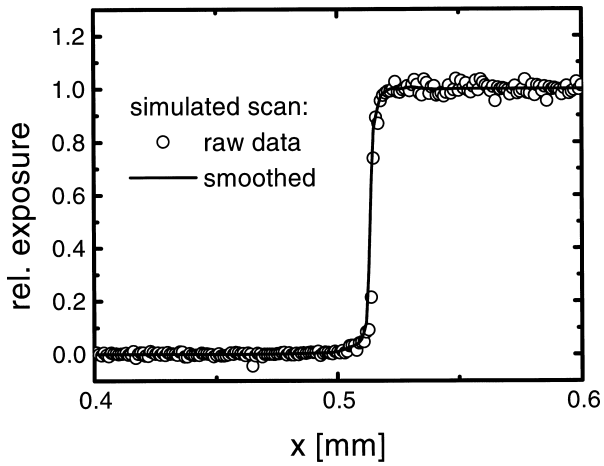

Figure 13. Simulated edge scan.

scanned by the simulated microdensitometer (200 slit-shaped pixels 1 μm × 500 μm, scanning distance 1 μm, green filter, configuration see Fig. 4). The microdensities $D(x)$ were then converted into relative exposures $E_{rel}(x)$ (Fig. 13) using the characteristic curve $D(\log E)$ of the simulated photographic process shown in Fig. 12.

(iv) Noise Removal. The edge scan in Fig. 13 resulting from the simulation of the complete photographic process (i) - (iv), is distorted by fluctuations due to the small areas considered. Therefore, a smoothing algorithm with a variable filter window is necessary. Away from the edge, up to 100 sampling points can be averaged but in the region around the edge only 3 sampling points are used. Figures 13 and 14 show an edge image and MTF, respectively, calculated with and without noise removal.

For both emulsions in Fig. 14, there is a good agreement between calculated and measured MTF. The small deviations can be attributed to the influence of noise in both measurement and also simulation.

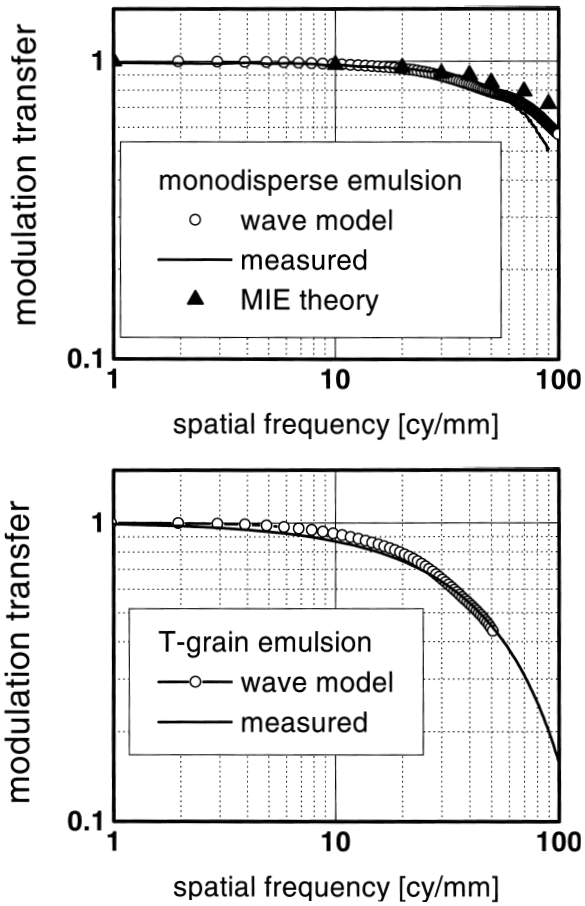

Figure 14. Comparison between calculated and measured MTF: monodisperse (a) and T-grain emulsion 0.8 μm (b).

Summary

Newly developed multiple-grid algorithms greatly reduce the computation times needed to calculate approximations of the light wave propagation in the vicinity of a grain of arbitrary shape from the Maxwell field equations. Rather than the 6 months estimated as necessary for conventional numerical methods, computation now can take about 8 h for 10^6 grid points in a volume element of $(2\ \mu m)^3$.

This is achieved by substituting a novel wave model for the Mie model when calculating the cross section of extinction, absorption probability, angular distribution and cross-section of light scattering for the silver halide grains. After introducing the layer structure and grain distribution of the real film into the model, light distribution and internal exposure can be calculated. Further steps in the model are the simulation of latent image formation and detection followed by the measurement of spatial microdensity distribution by microdensitometry.

It is now possible to simulate exposures for areas up to 200 μm × 500 μm. A novel method of removing granularity from both simulated and measured MTF test scans has been developed.

Acknowledgments. The authors thank the Deutsche Forschungsgemeinschaft for funding, and Kodak Limited Harrow, England, and Agfa-Gevaert AG Leverkusen, Germany, for providing the model emulsions used in this study.

References

1. D. Hertel and U. Siemen, Computer simulation of photon propagation in photographic emulsion layers, *J. Phot. Sci.* **44,** 2 (1996).
2. D. Hertel and U. Siemen, Computer simulation of photographic image recording, *Proc. of IS&T's 49th Annual Conference*, IS&T, Springfield, VA, 1996, p. 182.
3. S. Asano and G. Yamamoto, Light scattering by a spheroidal particle, *Appl. Opt.* **14,** 29 (1975).
4. S. Asano, Light scattering properties of spheroidal particles, *Appl. Opt.* **18,** 712 (1979).
5. V. Kurtz and S. Salib, Scattering and absorption of electromagnetic radiation by spheroidally shaped particles: Computation of the scattering properties, *J. Imaging Sci. Technol.* **37,** 43 (1993).
6. C. F. Bohren and D. R. Huffman, *Absorption and Scattering of Light by Small Particles*, New York, 1983.
7. Y. Luh, *Diskretisierungen und Mehrgitteralgorithmen zur Lösung hyperbolischer Differentialgleichungen, am Beispiel der Wellengleichung*, PhD thesis, University of Bonn, Germany, 1992.
8. H.-J. Metz, Zur Berechnung der Streulichtverteilung in photographischen Schichten, *Phot. Korr.* **106,** pp. 37, 56, 70 (1970).
9. K. Töpfer, J. R. Jarvis and D. Hertel, Physical and chemical properties of colour couplers in relation to the image quality of colour negative films, *J. Phot. Sci.* **42,** 149 (1994).
10. D. Hertel, K. Töpfer and H. Böttcher, Image quality investigations by means of photodetector arrays, *J. Imaging Sci. Technol.* **38,** 44 (1994).
11. J. J. DePalma and J. Gasper, Determining the optical properties of photographic emulsions by the Monte-Carlo method, *J. Phot. Sci. Eng.* **16,** 181 (1972).
12. E. Klein, Untersuchung der Streuung photographischer Schichten, *Phot. Korr.* **93,** 51 (1957).
13. H.-J. Metz, Extinktionsmessungen an monodispersen Suspensionen würfelförmiger AgBr-Teilchen, *Phot. Korr.* **99,** 153 (1963).
14. C. R. Berry, Turbidity of Monodisperse Suspensions of AgBr, *J. Opt. Soc. Am.* **52,** 888 (1962).